Multi-Objective Optimization for Customer Flexibility Management to Mitigate Consecutive Days of Power Supply Shortages

Yunchu Wang, *Student Member, IEEE,* Feng Lu, Chenghong Gu, *Member, IEEE,* Li Yang, *Member, IEEE,* Zhenzhi Lin, *Senior Member, IEEE*, Ming Wu, Liangzhong Yao, *Fellow, IEEE*

***Abstract*--Extreme weather such as heatwaves increases the probability of power system supply shortages, thus necessitating enhanced customer flexibility in instances of limited generation-side resources. This paper proposes an optimization model for managing customer flexibility to tackle multiple consecutive days of power supply shortages. Firstly, it constructs a customer flexibility management framework, considering power supply shortages under extreme heatwave conditions. Then, a multi-objective optimization is built for the customer flexibility management center to minimize the customer flexibility management costs and impacts on industrial customers' production. In this model, the impact index and customer uncertainty updating methods are proposed for managing customer flexibility over consecutive days based on exponential smoothing and Bayesian inference methods. A combined Tchebycheff decomposition and the analytic hierarchy process (AHP)-entropy weight method is constructed to tackle the impact of subjective and objective factors on decision-making. Finally, industrial customers in a city of Zhejiang province, China are used for case studies and the result shows that the proposed model can help customer flexibility management centers reduce and delay the power supply shortages during consecutive days of heatwaves.**

***Index Terms*--Customer Flexibility, Consecutive Days, Power Supply Shortages, Multi-Objective Optimization**

NOMENCLATURE

Decision Variables

$V_{i,d}^{\mathrm{I}}$	Combining the impact index of customer i for the optimization on day d
$V_{i,d}^{\mathrm{IH}}$	Impact index of customer i on day d
$P_{\mathrm{P},i,d,t}$	Peak-shaving demand response (DR) load
$P_{\mathrm{V},i,d,t}$	Valley-filling DR load
$v_{i,d,t}$	DR start state of customer i at time t on day d
$v_{\mathrm{P},i,d,t}$	DR start state of peak-shaving DR
$v_{\mathrm{V},i,d,t}$	DR start state of valley-filling DR
$l_{i,d,t}$	Invitation confirmation state of customer i
C_d^{W}	Customer flexibility management cost
C_d^{I}	Impact index on production of industrial customers
$P_{\mathrm{P},d,t}^{\mathrm{m}}$	Reduced power of flexible loads
$P_{V,i,d}^{\mathrm{c}}$	Capacity of valley-filling DR of industrial customer i
$P_{d,t}^{\mathrm{L}}$	Loss of load
$u_{i,d,t}$	DR invitation state of customer i
$u_{\mathrm{P},i,d,t} / u_{\mathrm{V},i,d,t}$	Peak-shaving/valley-filling DR state of customer i
$z_{\mathrm{P},i,d,t} / z_{\mathrm{V},i,d,t}$	Recovery state of peak-shaving/valley-filling DR of customer i
$T_{\mathrm{P},i,d,t}^{\mathrm{on}} / T_{\mathrm{V},i,d,t}^{\mathrm{on}}$	DR duration of peak-shaving/valley-filling DR of customer i
$T_{\mathrm{P},i,d,t}^{\mathrm{off}} / T_{\mathrm{V},i,d,t}^{\mathrm{off}}$	DR interval time of peak-shaving/valley-filling DR of customer i
$P_{\mathrm{P},i,d,t}^{*} / P_{\mathrm{V},i,d,t}^{*}$	Actual adjusted load of peak-shaving/valley-filling DR of customer i
$g_t / h_{i,t}$	Dual variables of the robust dual transformation
f_i	Multi-objectives of the customer flexibility management model
f_i^{OP}	Ideal objective of f_i
α_i	Weight factor of f_i
f_i^{NE}	Negative ideal objective of f_i
$a_i^{\mathrm{S}} / a_i^{\mathrm{O}}$	Subjective/objective weights of f_i
H	Deviation of subjective and objective weights
ω	Weight allocation coefficient
a_i^{B}	Optimal combination weight
$m_{\mathrm{I/II/III},i}$	Selection states for segments I, II, and III
F_i	Total profit losses for industrial customer i
F_i^{PC}	Profit losses in industrial process
F_i^{DR}	Income of DR for industrial customer i
$F_i^{\mathrm{ESS}} / F_i^{\mathrm{EGS}}$	Cost of energy storage system (ESS)/on-site energy generation system (EGS)

This work was supported by the Joint Fund of National Natural Science Foundation of China (No. U2166206). (*Corresponding author: Zhenzhi Lin.*)

Y. Wang is with the College of Electrical Engineering, Zhejiang University, Hangzhou 310027, China, and also with the Department of Electrical and Electronic Engineering, University of Bath, Bath BA2 7AY, U.K. (e-mail: wangyunchu_ee@zju.edu.cn).

F. Lu, L. Yang, and Z. Lin are with the College of Electrical Engineering, Zhejiang University, Hangzhou 310027, China. (e-mail: lu-feng@zju.edu.cn; eeyangli@zju.edu.cn; linzhenzhi@zju.edu.cn).

C. Gu is with the Department of Electrical and Electronic Engineering, University of Bath, Bath BA2 7AY, U.K. (e-mail: cg277@bath.ac.uk).

M. Wu is with the China Electric Power Research Institute, Beijing 100192, China. (e-mail: wuming@epri.sgcc.com.cn).

L. Yao is with the School of Electrical Engineering and Automation, Wuhan University, Wuhan 430072, China. (e-mail: yaoliangzhong@whu.edu.cn).

$E_{i,m,t}$	Storage of product resources m at time t
$x_{i,s,t}^{\mathrm{PC}}$	Reduced demand of task s at time t
$z_{i,s,t}^{\mathrm{PC}}$	Shutdown state of task s at time t
$P_{i,t}^{\mathrm{cha}} / P_{i,t}^{\mathrm{dis}}$	Charging/Discharging power of ESS
$P_{i,t}^{\mathrm{EGS}}$	Output power of EGS
$v_{i,t}^{\mathrm{EGS}} / z_{i,t}^{\mathrm{EGS}}$	Startup/Shutdown state of EGS
$E_{i,m,t}$	Storage of product resources m at time t
$R_{i,m,s}$	Input and output amount for product resources m in task s
$u_{i,s,t}^{\mathrm{PC}}$	Operation state of task s at time t
$v_{i,s,t}^{\mathrm{PC}} / z_{i,s,t}^{\mathrm{PC}}$	Startup/Shutdown state of task s at time t
$T_{i,s,t}^{\mathrm{PC,on}} / T_{i,s,t}^{\mathrm{PC,off}}$	Durations of task s in the on and off states
$S_{i,t}^{\mathrm{ESS}}$	State of charge (SOC) of ESS at time t
$u_{i,t}^{\mathrm{EGS}}$	Commitment state of EGS

Input Parameters

T	Number of time periods.
N_D	Number of customers
M_B	A large constant
M_{S}	A minimal constant
ρ^{H}	Weight parameter in exponential smoothing method
$a_{\mathrm{I/II/III},i}$	Coefficients of the linear terms for segments I, II, and III
$b_{\mathrm{II/III},i}$	Constant terms for segments II and III
$c_{\mathrm{I/II/III},i}$	Interruption costs for segments I, II, and III
$k_{\mathrm{I/II},i}$	Boundary points of the piecewise function
k	Maximum number of failures
$\lambda_{i,d}$	Participation uncertainty of customer i
∂_{D}	Limit of the failure reliability of all customers
$\alpha_{i,d}^{\mathrm{B}} / \beta_{i,d}^{\mathrm{B}}$	Parameters of the prior distribution of customer i
$\alpha_{i,0}^{\mathrm{B}} / \beta_{i,0}^{\mathrm{B}}$	Initial values of the prior distribution
$\mu_{i,0}^{\mathrm{H}}$	Number of invitation confirmations in the historical DR data
$\varepsilon_{i,0}^{\mathrm{H}}$	Number of invitation refusing in the historical DR data
$c_{\mathrm{P},i,t}^{\mathrm{p}}$	Unit electricity price for the peak-shaving DR of industrial customer i
$c_{\mathrm{P}}^{\mathrm{m}}$	Unit electricity price for flexible loads
$c_{\mathrm{V},i}^{\mathrm{c}}$	Unit capacity price for valley-filling DR of industrial customer i
c^{L}	Value of the lost load
$P_{d,t}^{\mathrm{DSM}}$	DR requirement of the customer flexibility management center
$R_{i,t}^{\mathrm{DRP}}$	Flexibility potential of customer i
$P_{i,\max}$	Maximum capacity of industrial customer i
$R_t^{U_i}$	Unit flexibility potential of customers with typical power consumption patterns
U_i	Typical power consumption patterns
$P_{\max,t}^{\mathrm{m}}$	Maximum flexibility capacity of flexible loads
$T_{\mathrm{P},i,\max}^{\mathrm{on}}$	Maximum DR duration of peak-shaving DR
$T_{\mathrm{V},i,\max}^{\mathrm{on}}$	Maximum DR duration of valley-filling DR
$T_{\mathrm{P},i,\min}^{\mathrm{on}}$	Minimum DR duration of peak-shaving DR
$T_{\mathrm{V},i,\min}^{\mathrm{on}}$	Minimum DR duration of valley-filling DR
$T_{\mathrm{P},i,\min}^{\mathrm{off}}$	Minimum interval time of peak-shaving DR
$T_{\mathrm{V},i,\min}^{\mathrm{off}}$	Minimum interval time of valley-filling DR
$U_{\max,i}^{\mathrm{d}}$	Maximum number of DR times in a single day
$U_{\max,i}^{\mathrm{M}}$	Maximum number of DR times during a month
$c_{i,m}^{\mathrm{F}}$	Unit value of the final product resources m
$E_{i,m}^{\mathrm{F}}$	Demand of the final product resources m
$c_{\mathrm{C},i,s}^{\mathrm{PC}}$	Unit cost for reduced demand of task s
$c_{\mathrm{I},i,s}^{\mathrm{PC}}$	Interrupt cost of task s
$c_{\mathrm{F},i}^{\mathrm{EGS}} / c_{\mathrm{U},i}^{\mathrm{EGS}}$	Fuel cost/Startup and shutdown cost of EGS
$N_{\mathrm{M},i}$	Total number of product resources
$N_{\mathrm{S},i}$	Total number of tasks
$P_{i,s}^{\mathrm{PC}}$	Power requirement for task s
$x_{0,i,s,t}^{\mathrm{PC}}$	Initial product demand of task s at time t.
$E_{i,m,\min}$	Lower storage limits of product resources m
$E_{i,m,\max}$	Upper storage limits of product resources m
$x_{0,i,s,\max}^{\mathrm{PC}}$	Maximum product demands for task s
$x_{0,i,s,\min}^{\mathrm{PC}}$	Minimum product demands for task s
$T_{i,s,\min}^{\mathrm{PC,on}}$ $T_{i,s,\max}^{\mathrm{PC,on}}$	Lower/Upper limits of the continuous operating time for task s
$T_{i,s,\min}^{\mathrm{PC,off}}$ $T_{i,s,\max}^{\mathrm{PC,off}}$	Lower/Upper limits of the operation interval time for task s
M_i^{ESS}	Capacity of ESS
$\eta_i^{\mathrm{cha}} / \eta_i^{\mathrm{dis}}$	Charging/Discharging efficiencies
$P_{i,\max}^{\mathrm{cha}} / P_{i,\max}^{\mathrm{dis}}$	Upper limit of the charging/discharge power
$S_{i,\min}^{\mathrm{ESS}} / S_{i,\max}^{\mathrm{ESS}}$	Lower/Upper limits of the SOC of ESS
$P_{i,\min}^{\mathrm{EGS}} / P_{i,\max}^{\mathrm{EGS}}$	Lower/Upper generation limit of EGS

I. INTRODUCTION

IN recent years, China's electricity consumption and peak demand have shown rapid growth. At the same time, factors such as rising primary energy costs and reduced hydroelectric power availability have constrained the power supply. These multifaceted impacts on both the power supply and demand sides have created a complex and challenging electricity supply and demand balance. Meanwhile, the continuous rise in global average temperature has further increased the demand. From 2021 to 2023, multiple regions, including western North America [1], Europe [2], and the eastern and northern parts of China experienced several heatwaves, resulting in multiple days of supply shortages. In the summer of 2022, during the extreme heatwave, approximately 20 provinces in China experienced power supply shortages [3]. Typically, heatwaves last between 3 to 5 days or 12 to 15 days, but this particular heatwave lasted nearly two months. The drought led to a reduction in hydroelectric power supply in provinces such as Sichuan, and the increase in electricity load, primarily due to air conditioning, resulted in prolonged power supply shortages in several regions. However, during consecutive days of scheduling, there was also a shortage of demand-side flexible resources, necessitating administrative measures to reduce electricity consumption. Hence, when the quantity of demand-side flexible resources is limited, optimizing customer flexibility to accommodate multiple days of supply shortages becomes a pressing concern.

Currently, demand response (DR) for commercial and industrial loads have been extensively developed in various countries and regions around the world to improve customer flexibility, and the DR programs in the power system can be divided into price-based DR and incentive-based DR [4]. When a potential power supply shortage is predicted at the day-ahead stage, the incentive-based DR, such as emergency DR and interruptible loads [5], is typically employed for customer flexibility management. For customer flexibility management centers, it is generally necessary to consider factors such as DR price, load characteristics, and customer satisfaction to optimize customer flexibility. In [6]-[7], the interruptible and curtailable loads were modeled based on the price elasticity of demand to formulate the participation of customers in DR programs. In [8]-[9], the data-driven Stackelberg game strategy is proposed for a distribution market operator to coordinate power dispatch among load aggregators. In [10], the stochastic optimization model considering flexible load resources coordinated control strategies for aggregated resources was developed, and the priority-list-based scheduling algorithm for each load type was proposed to allocate the resulting power trajectory to individual loads. For industrial load flexibility, the flexibility potential in industries and the applications of DR in the industrial sector were introduced in [11]. In [12], a multi-agent-based DR strategy coordinating the residential and industrial customers aggregators was proposed, and the flexibility potential of cement manufacture and metal smelting industries is considered in this model. In [13], the optimal scheduling model in industrial parks based on a load disaggregation algorithm was proposed to promote the profit of demand response aggregators. In [14], a real-time price-based DR algorithm is proposed for industrial facilities to minimize electricity costs while satisfying production requirements. The studies mentioned above have constructed customer flexibility optimization models primarily considering the response to pricing and the physical constraints of customers loads. However, these optimization models are limited to day-ahead and real-time time scales and do not take customer satisfaction into account.

Given that DR can potentially disrupt established electricity consumption patterns among customers, it is necessary to consider the impact on production or customer satisfaction in the customer flexibility optimization. In [15], a DR energy management scheme for industrial facilities based on the state task network was proposed to maximize the profit of industrial facilities. In [16], an industrial load control optimization model was proposed to maximize the profit of the steel mill industry, considering the behind-the-meter renewable generator and energy storage. In [17], a model predictive control method for cement plants participating in ancillary services was proposed. The above research considered the production processes of industrial customers and analyzed the impact of DR on production. However, the optimization model primarily focuses on maximizing the benefits for industrial customers, without accounting for the flexibility management of the power system. In [18], a multi-objective DR optimization model considering customers' satisfaction was proposed, and the absolute value of the difference between the electricity consumption before and after the proposed electricity price is normalized to quantify customer's satisfaction with the electricity consumption mode. In [19], fuzzy processing is utilized to transform the multi-objective optimization problem of considering customer satisfaction and microgrid operating costs into a single-objective problem. In [20], the customer DR satisfaction was utilized as a constraint in the day-ahead and real-time scheduling optimization model, and the customer way-of-use satisfaction and the customer cost satisfaction were combined into comprehensive satisfaction. In [21], customer satisfaction was described in terms of the actual power availability of each production process, and the NSGA-II algorithm was used to solve the multi-objective DR optimization model for load aggregators. The above research considered the impact of DR on production, as well as characteristics of customer participation uncertainty. However, customers' DR characteristics could be influenced by consecutive days of power supply shortages, and the customer flexibility management considering single days of requirements may result in insufficient responses during sustained extreme weather conditions.

Given this background, considering the variability in customer characteristics, the multi-objective optimization for customer flexibility management to mitigate consecutive days of power supply shortages is proposed in this paper. The major contributions of this work can be summarized as follows.

(1) To tackle consecutive days of power supply shortages during extreme weather conditions, a multi-objective optimization for managing customer flexibility that considers the consecutive impacts on customers' production is proposed. In the model, an exponential smoothing-based data updating method for the impact index is proposed. This ensures a more equitable distribution of flexibility management among customers, reducing the potential for load loss due to consecutive days of power supply shortages.

(2) An industrial customers' participation uncertainty updating and modeling method based on Bayesian inference and an improved *N-k* uncertainty set is proposed. The improved *N-k* uncertainty set with the parameters of customers' uncertainty could accommodate the differences in uncertainty across different customers and the variability in a single customer's uncertainty over consecutive days of power supply shortages. By updating customer characteristics throughout a long timescale, this approach can reduce the risk of load loss attributed to changes in customer uncertainty and improve the customer flexibility over a more extended period.

The rest of this paper is organized as follows. In Section II, the framework of consecutive days customer flexibility management is proposed. The multi-objective customer flexibility optimization model is presented in Section III. Case studies on customers in Zhejiang province, China, are presented in Section IV. Finally, the paper is concluded in Section V.

II. Framework of Customer Flexibility Management for Consecutive Days of Power Supply Shortages

A. Consecutive days of power supply shortages during extreme weather

Taking the heatwave in China from July to August 2022 as an example, an analysis of the power system's supply and demand situation under high-temperature weather is conducted. The maximum temperatures and power loads in Zhejiang province, China, during the heatwave from July 10 to July 16, 2022, are shown in Fig. 1. It can be seen from the figure that the maximum temperatures were above 36°C throughout the week, and the peak demand increased by 10.5% compared to a typical summer scenario. The generation capacity in Fig. 1(a) includes the maximum output of thermal, nuclear, hydro, wind, and photovoltaic power generation resources and the power that can be supplied from outside the province through transmission lines. The power supply shortage is part of the power load exceeding the generation capacity, which requires customer flexibility resources such as interruptible loads and translatable loads to maintain the balance of power supply and demand. As shown in Fig. 1(b), there was a power supply shortage every day from July 10 to July 16, accounting for 3.02% of the power load. The highest power supply shortage was 5525.34MW at 22:00 on July 14, accounting for 6.27% of the total load. Therefore, when there is a continuous daily power supply shortage, it is necessary for customer flexibility management centers to coordinate and schedule the limited demand-side flexible resources to secure the power supply for critical loads.

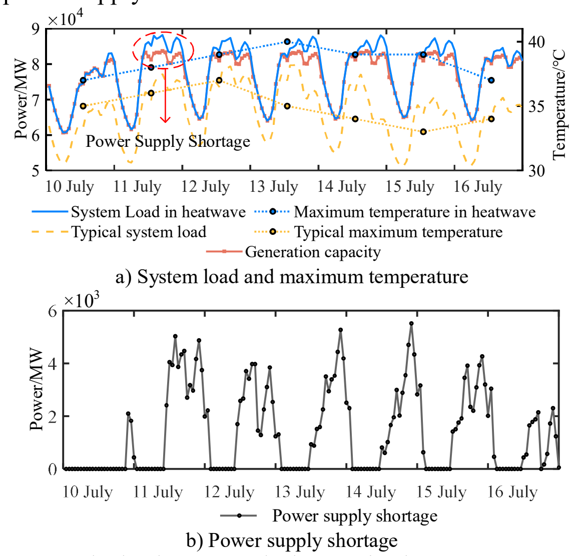

Fig. 1. System load and power supply shortages in a heatwave.

B. Framework for managing customer flexibility over consecutive days

Since 2022, China's Independent System Operator (ISO) has established multi-level customer flexibility management centers for provinces, cities, and counties [22]. When a potential power supply shortage is predicted at the day-ahead stage, the ISO will allocate the requirements to the lower-level customer flexibility management centers based on factors such as the total load in different areas. These customer flexibility management centers are responsible for managing the controllable load in their area, ensuring that the load reduction is equal to or greater than the power supply shortage.

The customer flexibility management execution procedure generally includes requirements confirmation, customer invitation, result evaluation and disclosure, and rewards release. Currently, the loads accessed to the customer flexibility management system include industrial and flexible loads such as electric vehicles and air conditioning. Among these, industrial customers can sign DR contracts with the customer flexibility management center, which include two types of DR methods: peak shaving DR and valley filling DR. The contracts specify customer flexibility management parameters for each industrial customer, including available periods for peak shaving DR and valley filling DR, electricity price for peak shaving DR, capacity price for valley filling DR, and the maximum number of DR per day and month. The industrial customer can confirm the invitation at the DR scheduling and customer invitation stage, and the customer flexibility management execution could be carried out through the customer flexibility management system. The adjusted loads are equal to their flexibility potential, which can be obtained by flexibility potential evaluation methods [23]. Besides, industrial customers can refuse the invitation if they believe DR significantly impacts their production. Meanwhile, the customer flexibility management center can directly control flexible loads, reducing electricity consumption through the customer flexibility management system, but it is subject to a maximum capacity limit.

The framework of the customer flexibility optimization over consecutive days is illustrated in Fig. 2. At the day-ahead stage of day *d*, the customer flexibility management center receives the requirement from the ISO. When the customer flexibility management is conducted over several consecutive days, the instances of industrial customers refusing the invitation increase, leading to the inability to meet requirements. It is necessary to consider the impacts on production and the variability in customer uncertainty to optimize customer flexibility. Therefore, the multi-objective optimization model is built for the customer flexibility management center to minimize customer flexibility management costs and the impact on production. In this model, customer flexibility management costs include the electricity cost of peak-shaving DR and the capacity cost of valley-filling DR for industrial loads, as well as the electricity cost for flexible loads adjustment. The impact on industrial production is modeled as a three segments piecewise function based on the resource-task network (RTN) model. Considering the effects of consecutive days management, the impact index used in decision-making needs to be calculated by combining the impact index for day *d* with the historical impact index. Meanwhile, considering the changes in customers uncertainty and the differences in uncertainty among different industrial customers, an improved *N-k* uncertainty is used to handle the different customer participation uncertainty. Consequently, data updating is required before the customer flexibility management on day d. The customers' participation uncertainty and impact index could be updated based on the new results obtained from the customer flexibility management on day d-1. Similarly, the results from the customer flexibility management on day d are also utilized for the customer flexibility optimization on day d+1.

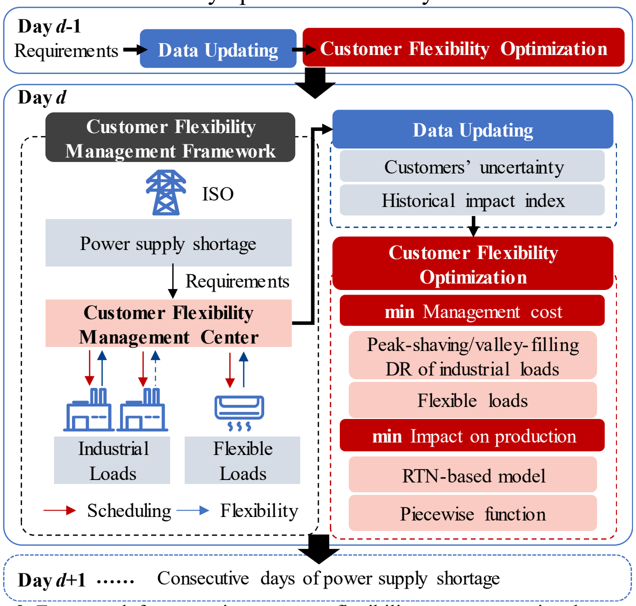

Fig. 2. Framework for managing customer flexibility over consecutive days.

III. Multi-Objective Customer Flexibility Optimization Model for Multiple Consecutive Days

A. Impacts index for consecutive days of flexibility management on industrial production

In extreme weather, such as persistent high temperatures, the power systems may have the customer flexibility management requirements for several days, and the adjustable load of the same customer will inevitably be reduced many times in a single day or multiple consecutive days. The impact on the production of these industrial customers after participating in customer flexibility management is an essential factor affecting the management quantity of the customer flexibility management center. The impacts on industrial production are mainly related to the number of interruptions and the rate of electricity reduction. For the customer flexibility management over consecutive days, the impact index used in the optimization model needs to be calculated by combining the impact index for day d with the historical impact index. Considering the decreasing influence of historical customer flexibility management on the current day, the exponential smoothing (ES) method can be utilized to obtain a weighted average of the impact index [24]. Therefore, the impact index on industrial production considering consecutive days of customer flexibility management can be expressed as

$$V_{i,d}^{\mathrm{I}} = \rho^{\mathrm{H}} V_{i,d}^{\mathrm{IH}} + (1-\rho^{\mathrm{H}}) V_{i,d-1}^{\mathrm{I}} \tag{1}$$

where $V_{i,d}^{\mathrm{I}}$ is the combining impact index of customer i for the optimization on day d, and $V_{i,0}^{\mathrm{I}} = 0$. $V_{i,d}^{\mathrm{IH}}$ is the impact index of customer i on day d. ρ^{H} is the weight parameter in ES, and $\rho^{\mathrm{H}} \in [0.5,1]$. When $\rho^{\mathrm{H}} = 1$, the impact index only considers the previous day.

To determine the complex impacts of flexibility management on industrial production, the RTN-based flexibility management model for industrial customers can be developed. In the RTN-based model, the variables and constraints are written in terms of abstract entities like resources, tasks, and event points [25]. Additionally, the on-site energy generation system (EGS) and energy storage system (EES) are modeled for decreasing the impacts on industrial production. The optimization objective is to minimize the profit losses for the industrial customer, which can be expressed as

$$\min F_i = F_i^{\mathrm{PC}} - F_i^{\mathrm{DR}} + F_i^{\mathrm{ESS}} + F_i^{\mathrm{EGS}} \tag{2}$$

$$\begin{aligned} F_i^{\mathrm{PC}} = & \sum_{m=1}^{N_{\mathrm{M},i}} c_{i,m}^{\mathrm{F}} \max(E_{i,m}^{\mathrm{F}} - E_{i,m,T}, 0) \\ & + \sum_{t=1}^{T} \sum_{s=1}^{N_{\mathrm{S},i}} (x_{i,s,t}^{\mathrm{PC}} c_{\mathrm{C},i,s}^{\mathrm{PC}} + z_{i,s,t}^{\mathrm{PC}} c_{\mathrm{I},i,s}^{\mathrm{PC}}) \end{aligned} \tag{3}$$

$$F_i^{\mathrm{DR}} = \sum_{t=1}^{T} c_{\mathrm{P},i,t}^{\mathrm{p}} P_{\mathrm{P},i,d,t} + c_{\mathrm{V},i}^{\mathrm{c}} P_{\mathrm{V},i,d}^{\mathrm{c}} \tag{4}$$

$$F_i^{\mathrm{ESS}} = \sum_{t=1}^{T} c_i^{\mathrm{ESS}} (P_{i,t}^{\mathrm{cha}} + P_{i,t}^{\mathrm{dis}}) \tag{5}$$

$$F_i^{\mathrm{EGS}} = \sum_{t=1}^{T} c_{\mathrm{F},i}^{\mathrm{EGS}} P_{i,t}^{\mathrm{EGS}} + \sum_{t=1}^{T} c_{\mathrm{U},i}^{\mathrm{EGS}} (v_{i,t}^{\mathrm{EGS}} + z_{i,t}^{\mathrm{EGS}}) \tag{6}$$

where F_i is the total profit losses for industrial customer i. F_i^{PC} is the profit losses in industrial process for industrial customer i, which is combined with the final product resources losses and the cost of task interruption. F_i^{DR} is the income of DR for industrial customer i. F_i^{ESS} and F_i^{EGS} are the cost of ESS and EGS, respectively. $c_{i,m}^{\mathrm{F}}$ is the unit value of the final product resources m. $E_{i,m}^{\mathrm{F}}$ is the demand of the final product resources m. $E_{i,m,T}$ is the storage of product resources m at time T. $x_{i,s,t}^{\mathrm{PC}}$ is the reduced demand of task s at time t. $c_{\mathrm{C},i,s}^{\mathrm{PC}}$ is the unit cost for reduced demand of task s. $z_{i,s,t}^{\mathrm{PC}}$ is the shutdown state of task s at time t. $c_{\mathrm{I},i,s}^{\mathrm{PC}}$ is the interrupt cost of task s. $P_{i,t}^{\mathrm{cha}}$ and $P_{i,t}^{\mathrm{dis}}$ are the charging and discharging power of ESS at time t. c_i^{ESS} is the degradation cost of ESS. $P_{i,t}^{\mathrm{EGS}}$ is the output power of EGS. $c_{\mathrm{F},i}^{\mathrm{EGS}}$ and $c_{\mathrm{U},i}^{\mathrm{EGS}}$ are the fuel cost and the startup/shutdown cost of EGS, respectively. $v_{i,t}^{\mathrm{EGS}}$ and $z_{i,t}^{\mathrm{EGS}}$ are the startup and shutdown state of EGS at time t, respectively. $N_{\mathrm{M},i}$ is the total number of product resources for industrial customer i. $N_{\mathrm{S},i}$ is the total number of tasks for industrial customer i.

Constraints of RTN-based flexibility management model for industrial customers include the power balance constraint, process flow constraints, ESS operation constraints, and EGS operation constraints, which can be expressed as follows.

1) Power balance constraint

$$P_{\mathrm{P},i,d,t} - P_{\mathrm{V},i,d,t} = P_{i,t}^{\mathrm{EGS}} + P_{i,t}^{\mathrm{dis}} - P_{i,t}^{\mathrm{cha}} + \sum_{s=1}^{N_{\mathrm{S}}} P_{i,s}^{\mathrm{PC}} x_{i,s,t}^{\mathrm{PC}} \tag{7}$$

where $P_{i,s}^{\mathrm{PC}}$ is the power requirement for task s.

2) Process flow constraints

$$E_{i,m,t+1} = E_{i,m,t} + \sum_{s=1}^{N_{\mathrm{S},i}} R_{i,m,s}(x_{0,i,s,t}^{\mathrm{PC}} - x_{i,s,t}^{\mathrm{PC}}) \tag{8}$$

$$E_{i,m,\min} \le E_{i,m,t} \le E_{i,m,\max} \tag{9}$$

$$u_{i,s,t}^{\mathrm{PC}} x_{0,i,s,\min}^{\mathrm{PC}} \le x_{0,i,s,t}^{\mathrm{PC}} \le u_{i,s,t}^{\mathrm{PC}} x_{0,i,s,\max}^{\mathrm{PC}} \tag{10}$$

$$x_{i,s,\min}^{\mathrm{PC}} \le x_{i,s,t}^{\mathrm{PC}} \le x_{i,s,\max}^{\mathrm{PC}}, \forall s \in S^{\mathrm{ST}} \tag{11}$$

$$x_{i,s,t}^{\mathrm{PC}} = 0, \forall s \in S^{\mathrm{NST}} \tag{12}$$

$$u_{i,s,t}^{\mathrm{PC}} = 1, \forall s \in S^{\mathrm{NST}} \tag{13}$$

$$v_{i,s,t}^{\mathrm{PC}} + z_{i,s,t}^{\mathrm{PC}} \le 1 \tag{14}$$

$$u_{i,s,t}^{\mathrm{PC}} - u_{i,s,t-1}^{\mathrm{PC}} = v_{i,s,t}^{\mathrm{PC}} - z_{i,s,t}^{\mathrm{PC}} \tag{15}$$

$$T_{i,s,t}^{\mathrm{PC,on}} = u_{i,s,t}^{\mathrm{PC}}(T_{i,s,t-1}^{\mathrm{PC,on}} + 1) \tag{16}$$

$$T_{i,s,\min}^{\mathrm{PC,on}} z_{i,s,t}^{\mathrm{PC}} \le T_{i,s,t-1}^{\mathrm{PC,on}} \le T_{i,s,\max}^{\mathrm{PC,on}} \tag{17}$$

$$T_{i,s,t}^{\mathrm{PC,off}} = (1 - u_{i,s,t}^{\mathrm{PC}})(T_{i,s,t-1}^{\mathrm{PC,off}} + 1) \tag{18}$$

$$T_{i,s,\min}^{\mathrm{PC,off}} v_{i,s,t}^{\mathrm{PC}} \le T_{i,s,t-1}^{\mathrm{PC,off}} \le T_{i,s,\max}^{\mathrm{PC,off}} \tag{19}$$

where $E_{i,m,t}$ is storage of product resources m at time t. $R_{i,m,s}$ is the input and output amount for product resources m in task s. $x_{0,i,s,t}^{\mathrm{PC}}$ is the initial product demand of task s at time t. $E_{i,m,\min}$ and $E_{i,m,\max}$ are the lower and upper storage limits of product resources m. $x_{0,i,s,\max}^{\mathrm{PC}}$ and $x_{0,i,s,\min}^{\mathrm{PC}}$ are the maximum and minimum product demands for task s, respectively. $u_{i,s,t}^{\mathrm{PC}}$ is the operation state of task s at time t. $v_{i,s,t}^{\mathrm{PC}}$ and $z_{i,s,t}^{\mathrm{PC}}$ are startup and shutdown state of task s at time t, respectively. $T_{i,s,t}^{\mathrm{PC,on}}$ and $T_{i,s,t}^{\mathrm{PC,off}}$ are the durations of task s in the on and off states at time t, respectively. $T_{i,s,\min}^{\mathrm{PC,on}}$ and $T_{i,s,\max}^{\mathrm{PC,on}}$ are the lower and upper limits of the continuous operating time for task s, respectively. $T_{i,s,\min}^{\mathrm{PC,off}}$ and $T_{i,s,\max}^{\mathrm{PC,off}}$ are the lower and upper limits of the operation interval time for task s, respectively.

3) ESS operation constraints

$$S_{i,t}^{\mathrm{ESS}} M_i^{\mathrm{ESS}} = S_{i,t-1}^{\mathrm{ESS}} M_i^{\mathrm{ESS}}(1 - \psi_i^{\mathrm{ESS}}) + \eta_i^{\mathrm{cha}} P_{i,t}^{\mathrm{cha}} - P_{i,t}^{\mathrm{dis}} / \eta_i^{\mathrm{dis}} \tag{20}$$

$$0 \le P_{i,t}^{\mathrm{cha}} \le P_{i,\max}^{\mathrm{cha}}, \quad 0 \le P_{i,t}^{\mathrm{dis}} \le P_{i,\max}^{\mathrm{dis}} \tag{21}$$

$$S_{i,\min}^{\mathrm{ESS}} \le S_{i,t}^{\mathrm{ESS}} \le S_{i,\max}^{\mathrm{ESS}}, S_{i,0}^{\mathrm{ESS}} = S_{i,T}^{\mathrm{ESS}} \tag{22}$$

where $S_{i,t}^{\mathrm{ESS}}$ is the state of charge (SOC) of ESS at time t. M_i^{ESS} is the capacity of ESS. η_i^{cha} and η_i^{dis} are the charging and discharging efficiencies, respectively. $P_{i,\max}^{\mathrm{cha}}$ and $P_{i,\max}^{\mathrm{dis}}$ are the upper limit of the charging and discharge power of ESS. $S_{i,\min}^{\mathrm{ESS}}$ and $S_{i,\max}^{\mathrm{ESS}}$ are the lower and upper limits of the SOC of ESS, respectively.

4) EGS operation constraints

$$u_{i,t}^{\mathrm{EGS}} P_{i,\min}^{\mathrm{EGS}} \le P_{i,t}^{\mathrm{EGS}} \le u_{i,t}^{\mathrm{EGS}} P_{i,\max}^{\mathrm{EGS}} \tag{23}$$

$$v_{i,t}^{\mathrm{EGS}} + z_{i,t}^{\mathrm{EGS}} \le 1 \tag{24}$$

$$u_{i,t}^{\mathrm{EGS}} - u_{i,t-1}^{\mathrm{EGS}} = v_{i,t}^{\mathrm{EGS}} - z_{i,t}^{\mathrm{EGS}} \tag{25}$$

where $P_{i,\max}^{\mathrm{EGS}}$ and $P_{i,\min}^{\mathrm{EGS}}$ are the upper and lower generation limit of EGS, respectively. $u_{i,t}^{\mathrm{EGS}}$ is commitment state of EGS at time t.

The RTN-based model for industrial customers could be transformed into the Karush-Kuhn-Tucker (KKT) conditions and incorporated into the optimization model for customer flexibility management center. However, due to the fact that raw material costs, product revenues, and equipment parameters of different industrial customers are considered private, it is challenging for the customer flexibility management center to access specific model parameters. Therefore, through simulation and regression analysis, the relationship between production losses and reduced load of industrial customers is established and divided into three segments. The impact index of customer i on day d can be expressed as

$$V_{i,d}^{\mathrm{IH}} = \begin{cases} a_{\mathrm{I},i}\sum_{t=1}^{T} P_{\mathrm{P},i,d,t} + c_{\mathrm{I},i}\sum_{t=1}^{T} v_{i,d,t}, 0 \le \sum_{t=1}^{T} P_{\mathrm{P},i,d,t} \le k_{\mathrm{I},i} \\ a_{\mathrm{II},i}\sum_{t=1}^{T}(P_{\mathrm{P},i,d,t} - P_{\mathrm{V},i,d,t}) + b_{\mathrm{II},i} + c_{\mathrm{II},i}\sum_{t=1}^{T} v_{i,d,t} \\ \qquad , k_{\mathrm{I},i} \le \sum_{t=1}^{T} P_{\mathrm{P},i,d,t} \le k_{\mathrm{II},i} \\ a_{\mathrm{III},i}\sum_{t=1}^{T} P_{\mathrm{P},i,d,t} + b_{\mathrm{III},i} + c_{\mathrm{III},i}\sum_{t=1}^{T} v_{i,d,t}, k_{\mathrm{II},i} \le \sum_{t=1}^{T} P_{\mathrm{P},i,d,t} \end{cases} \tag{26}$$

$$v_{i,d,t} = v_{\mathrm{P},i,d,t} + v_{\mathrm{V},i,d,t} \tag{27}$$

where $P_{\mathrm{P},i,d,t}$ and $P_{\mathrm{V},i,d,t}$ are the peak-shaving DR load and valley-filling DR load of customer i at time t on day d, respectively. $v_{i,d,t}$ is the DR start state of customer i at time t on day d, which is a binary variable, and $v_{i,d,t} = 1$ indicates that customer i starts to DR for peak-shaving or valley-filling at time t. $v_{\mathrm{P},i,d,t}$ and $v_{\mathrm{V},i,d,t}$ are the DR start state of peak-shaving and valley-filling DR of customer i at time t on day d, respectively. $a_{\mathrm{I},i}$, $a_{\mathrm{II},i}$, and $a_{\mathrm{III},i}$ are the coefficients of the linear terms for segments I, II, and III of the piecewise function, respectively. $b_{\mathrm{II},i}$ and $b_{\mathrm{III},i}$ are the constant terms for segments II and III, respectively. $c_{\mathrm{I},i}$, $c_{\mathrm{II},i}$, and $c_{\mathrm{III},i}$ are the interruption costs for segments I, II, and III of the piecewise function. $k_{\mathrm{I},i}$ and $k_{\mathrm{II},i}$ are the boundary points of the piecewise function. T is the number of time periods.

In segment I, the ESS and EGS can be used for power generation without impacting production. The losses for industrial customers participating in DR are primarily associated with the cost of ESS or ESG operation. When the reduced load exceeds the maximum capacity of ESS or EGS, or for customers without ESS or EGS, the production losses for industrial customers are divided into two segments (Segment II and Segment III). In segment II, the production line can still operate normally. The production losses during peak-shaving DR can be compensated by valley-filling DR. Here, production losses are mainly influenced by output reduction. In segment III, when the reduced load exceeds a specified threshold, the reduction in load may lead to the termination of an entire production line. In this case, production losses are directly proportional to the reduced load and exhibit a steep increase. In each segment, the interruption costs represent the startup and shutdown costs of the EGS, as well as the management costs associated with changes in the working hours of their production lines.

Based on Big-M method, the piecewise function of production impacts can be linearized, which can be respectively converted into

$$V_{i,d}^{\mathrm{IH}} \geq -M_{\mathrm{B}}(1-m_{\mathrm{I},i}) + a_{\mathrm{I},i}\sum_{t=1}^{T} P_{\mathrm{P},i,d,t} + c_{\mathrm{I},i}\sum_{t=1}^{T} v_{i,d,t} \tag{28}$$

$$V_{i,d}^{\mathrm{IH}} \leq M_{\mathrm{B}}(1-m_{\mathrm{I},i}) + a_{\mathrm{I},i}\sum_{t=1}^{T} P_{\mathrm{P},i,d,t} + c_{\mathrm{I},i}\sum_{t=1}^{T} v_{i,d,t} \tag{29}$$

$$\begin{aligned} V_{i,d}^{\mathrm{IH}} \geq & -M_{\mathrm{B}}(1-m_{\mathrm{II},i}) + a_{\mathrm{II},i}\sum_{t=1}^{T} (P_{\mathrm{P},i,d,t} - P_{\mathrm{V},i,d,t}) \\ & + b_{\mathrm{II},i} + c_{\mathrm{II},i}\sum_{t=1}^{T} v_{i,d,t} \end{aligned} \tag{30}$$

$$\begin{aligned} V_{i,d}^{\mathrm{IH}} \leq & M_{\mathrm{B}}(1-m_{\mathrm{II},i}) + a_{\mathrm{II},i}\sum_{t=1}^{T} (P_{\mathrm{P},i,d,t} - P_{\mathrm{V},i,d,t}) \\ & + b_{\mathrm{II},i} + c_{\mathrm{II},i}\sum_{t=1}^{T} v_{i,d,t} \end{aligned} \tag{31}$$

$$V_{i,d}^{\mathrm{IH}} \geq -M_{\mathrm{B}}(1-m_{\mathrm{III},i}) + a_{\mathrm{III},i}\sum_{t=1}^{T} P_{\mathrm{P},i,d,t} + b_{\mathrm{III},i} + c_{\mathrm{III},i}\sum_{t=1}^{T} v_{i,d,t} \tag{32}$$

$$V_{i,d}^{\mathrm{IH}} \leq M_{\mathrm{B}}(1-m_{\mathrm{III},i}) + a_{\mathrm{III},i}\sum_{t=1}^{T} P_{\mathrm{P},i,d,t} + b_{\mathrm{III},i} + c_{\mathrm{III},i}\sum_{t=1}^{T} v_{i,d,t} \tag{33}$$

$$k_{\mathrm{I},i}m_{\mathrm{I},i} + k_{\mathrm{II},i}m_{\mathrm{II},i} \leq \sum_{t=1}^{T} P_{\mathrm{P},i,d,t} \leq k_{\mathrm{I},i}m_{\mathrm{I},i} + k_{\mathrm{II},i}m_{\mathrm{II},i} + M_{\mathrm{B}}m_{\mathrm{III},i} \tag{34}$$

$$m_{\mathrm{I},i} + m_{\mathrm{II},i} + m_{\mathrm{III},i} = 1 \tag{35}$$

where $m_{\mathrm{I},i}$, $m_{\mathrm{II},i}$, and $m_{\mathrm{III},i}$ are respectively the selection states for segments I, II, and III, which are binary variables.

B. Customer participation uncertainty updating and modeling method based on Bayesian inference and an improved N-k uncertainty set

When industrial customers participate in DR, they can refuse the invitation if they believe the DR significantly impacts their production. Therefore, the *N-k* uncertainty set can represent the failure state of invitation confirmation.

1)*N-k* uncertainty set

The *N-k* uncertainty set is suitable for the robust optimization model for accidental failures [26] and can limit the number of industrial customers with actual DR through *N-k* constraints, which can be expressed as

$$L = \left\{ l \mid l_{i,d,t} \in \{0,1\}, \sum_{i=1}^{N_{\mathrm{D}}} l_{i,d,t} \geqslant N_{\mathrm{D}} - k \right\} \tag{36}$$

where $l_{i,d,t}$ is the invitation confirmation state of customer *i* at time *t* on day *d*. *k* is the maximum number of failures. N_D is the total number of customers.

The *N-k* uncertainty set restricts the number of customers for actual DR. However, the *N-k* uncertainty set does not consider differences in customer DR participation uncertainty. If an industrial customer with low level of participation uncertainty fails to DR, the *N-k* robust optimization may produce results that are significantly different from the actual situation. Conversely, when industrial customers have higher level of participation uncertainty, there may be scenarios where multiple industrial customers refuse the invitation simultaneously. Therefore, an improved *N-k* uncertainty set for customer participation uncertainty difference is constructed.

2) Improved *N-k* uncertainty set considering the participation uncertainty difference of customers

Based on the *N-k* uncertainty set, the improved *N-k* uncertainty set is constructed considering the participation uncertainty difference of customer flexibility resources. In this uncertainty set, $\lambda_{i,d}$ is the participation uncertainty of customer *i* on day *d*, which refers to the probability of the invitation being declined. ∂_{D} is the limit of the failure probability of all customers on day *d*. Therefore, the improved *N-k* uncertainty set can be expressed as

$$L^{*} = \left\{ l \mid l_{i,d,t} \in \{0,1\}, \prod_{i=1}^{N_{\mathrm{D}}} \lambda_{i,d}^{1-l_{i,d,t}} \prod_{i=1}^{N_{\mathrm{D}}} \left(1-\lambda_{i,d}\right)^{l_{i,d,t}} \geqslant \partial_{\mathrm{D}} \right\} \tag{37}$$

In this improved *N-k* uncertainty set, the participation uncertainty of customers has to be updated according to the result on day *d*-1, and a Bayesian inference-based data updating method is proposed. Since the customer's invitation confirmation state is a binary random variable, it can be represented by a Bernoulli distribution, with its prior distribution typically expressed as a Beta distribution [27]. The participation uncertainty of customers on day *d* can be updated with the prior probability beliefs and recent results, which can be expressed as

$$\lambda_{i,d} = 1 - \frac{\alpha_{i,d}^{\mathrm{B}}}{\alpha_{i,d}^{\mathrm{B}} + \beta_{i,d}^{\mathrm{B}}} \tag{38}$$

$$\alpha_{i,d}^{\mathrm{B}} = \alpha_{i,d-1}^{\mathrm{B}} + \sum_{t=1}^{\mathrm{T}} l_{i,d-1,t} \tag{39}$$

$$\beta_{i,d}^{\mathrm{B}} = \beta_{i,d-1}^{\mathrm{B}} + \sum_{t=1}^{T} u_{i,d-1,t} - \sum_{t=1}^{T} l_{i,d-1,t} \tag{40}$$

$$\alpha_{i,0}^{\mathrm{B}} = \mu_{i,0}^{\mathrm{H}} + 1, \beta_{i,0}^{\mathrm{B}} = \varepsilon_{i,0}^{\mathrm{H}} + 1 \tag{41}$$

where $\alpha_{i,d}^{\mathrm{B}}$ and $\beta_{i,d}^{\mathrm{B}}$ are two parameters of the prior distribution of customer *i* on day *d*. $\alpha_{i,0}^{\mathrm{B}}$ and $\beta_{i,0}^{\mathrm{B}}$ are the initial values, which can be calculated with the number of invitation confirmations $\mu_{i,0}^{\mathrm{H}}$ and the number of invitation refusing $\varepsilon_{i,0}^{\mathrm{H}}$ in the historical DR data of customer *i*. $u_{i,d,t}$ is the DR invitation state of customer *i* at time *t* on day *d*, including the peak-shaving and valley-filling DR state.

With the logarithm of the improved *N-k* uncertainty set, the participation uncertainty constraints can be expressed as

$$\sum_{i=1}^{N_{\mathrm{D}}} l_{i,d,t} \lg(1-\lambda_{i,d}) + \sum_{i=1}^{N_{\mathrm{D}}} \left(1-l_{i,d,t}\right) \lg \lambda_{i,d} \geqslant \lg \partial_{\mathrm{D}} \tag{42}$$

$$\sum_{i=1}^{N_{\mathrm{D}}} l_{i,d,t} \left(\lg\left(1-\lambda_{i,d}\right) - \lg \lambda_{i,d}\right) \geqslant \lg \partial_{\mathrm{D}} - \sum_{i=1}^{N_{\mathrm{D}}} \lg \lambda_{i,d} \tag{43}$$

C. Multi-objective optimization for managing customer flexibility considering impacts on industrial production

Considering the impacts on industrial production and the uncertainty of industrial customers' invitation confirmation, a multi-objective optimization model for managing customer flexibility over multiple consecutive days is constructed. In the optimization model for day *d*, the optimization objectives are to minimize customer flexibility management costs and the impact index on production, which can be expressed as

$$\min[f_1, f_2] = \min[C_d^{\mathrm{W}}, C_d^{\mathrm{I}}] \tag{44}$$

$$\begin{aligned} C_d^{\mathrm{W}} &= \sum_{i=1}^{N_{\mathrm{D}}}\left(\sum_{t=1}^{T} c_{\mathrm{P},i,t}^{\mathrm{p}} P_{\mathrm{P},i,d,t} + c_{\mathrm{V},i}^{\mathrm{c}} P_{\mathrm{V},i,d}^{\mathrm{c}}\right) \\ &+\sum_{t=1}^{T} c_{\mathrm{P}}^{\mathrm{m}} P_{\mathrm{P},d,t}^{\mathrm{m}} + \sum_{t=1}^{T} c^{\mathrm{L}} P_{d,t}^{\mathrm{L}} \end{aligned} \tag{45}$$

$$C_d^{\mathrm{I}} = \sum_{i=1}^{N_{\mathrm{D}}} V_{i,d}^{\mathrm{I}} \tag{46}$$

where C_d^{W} and C_d^{I} are the customer flexibility management cost of the customer flexibility management center and the impact index on production of industrial customers on day d, respectively. $c_{\mathrm{P},i,t}^{\mathrm{p}}$ is the unit electricity price for the peak-shaving DR of industrial customer i at time t on day d. $c_{\mathrm{P}}^{\mathrm{m}}$ is the unit electricity price for flexible loads. $c_{\mathrm{V},i}^{\mathrm{c}}$ is the unit capacity price for valley-filling DR of industrial customer i. $P_{\mathrm{P},d,t}^{\mathrm{m}}$ is the reduced power of flexible loads at time t on day d. $P_{V,i,d}^{\mathrm{c}}$ is the capacity of valley-filling DR of industrial customer i on day d. $P_{d,t}^{\mathrm{L}}$ is the loss of load, and $P_{d,t}^{\mathrm{L}} \geq 0$. c^{L} is the value of the lost load (VOLL).

Constraints of the customer flexibility optimization model include the power balance constraint, flexibility capacity constraints, DR duration constraints, DR interval time constraints, the maximum number of DR constraints, and customer uncertainty constraints, which can be expressed as follows.

1) Power balance constraint

When a potential power supply shortage is predicted in the power system, the total power of customer flexibility management needs to equal the DR requirement of the customer flexibility management center; otherwise, load loss will occur in the power system. The power balance constraint can be expressed as follows: The power balance constraint can be expressed as

$$\sum_{i=1}^{N_D} P_{\mathrm{P},i,d,t} - \sum_{i=1}^{N_D} P_{\mathrm{V},i,d,t} + P_{\mathrm{P},d,t}^{\mathrm{m}} = P_{d,t}^{\mathrm{DSM}} - P_{d,t}^{\mathrm{L}}, \forall P_{d,t}^{\mathrm{DSM}} > 0 \tag{47}$$

where $P_{d,t}^{\mathrm{DSM}}$ is the DR requirement of the customer flexibility management center at time t on day d.

2) Flexibility capacity constraints

For industrial customers confirming the invitation, the industrial loads are controlled by the customer flexibility management system, and the adjusted loads are equal to their flexibility potential. For flexible loads, the adjusted loads must be less than the maximum flexibility capacity. Therefore, the flexibility capacity constraints can be expressed as

$$P_{\mathrm{P},i,d,t} = u_{\mathrm{P},i,d,t} l_{i,d,t} R_{i,t}^{\mathrm{DRP}} \tag{48}$$

$$P_{\mathrm{V},i,d,t} = -u_{\mathrm{V},i,d,t} l_{i,d,t} R_{i,t}^{\mathrm{DRP}} \tag{49}$$

$$R_{i,t}^{\mathrm{DRP}} = P_{i,\max} R_t^{U_i} \tag{50}$$

$$P_{V,i,d}^{\mathrm{c}} \geq P_{\mathrm{V},i,d,t} \geq 0 \tag{51}$$

$$0 \leq P_{\mathrm{P},d,t}^{\mathrm{m}} \leq P_{\max,t}^{\mathrm{m}} \tag{52}$$

where $u_{\mathrm{P},i,d,t}$ and $u_{\mathrm{V},i,d,t}$ are the peak-shaving and valley-filling DR state of customer i at time t on day d, respectively, which are binary variables. $R_{i,t}^{\mathrm{DRP}}$ is the flexibility potential of customer i at time t. $P_{i,\max}$ is the maximum capacity of industrial customer i. $R_t^{U_i}$ is the unit flexibility potential of customers with typical power consumption patterns U_i . $P_{\max,t}^{\mathrm{m}}$ is the maximum flexibility capacity of flexible loads at time t.

3) DR duration constraints

As the duration of a single DR cannot exceed the upper limit in the customer flexibility management contract, and customers have the minimum interruption duration in some industrial processes, the upper and lower limits of the DR duration can be expressed as

$$v_{\mathrm{P},i,d,t} + z_{\mathrm{P},i,d,t} \leq 1, v_{\mathrm{V},i,d,t} + z_{\mathrm{V},i,d,t} \leq 1 \tag{53}$$

$$u_{\mathrm{P},i,d,t} - u_{\mathrm{P},i,d,t-1} = v_{\mathrm{P},i,d,t} - z_{\mathrm{P},i,d,t} \tag{54}$$

$$u_{\mathrm{V},i,d,t} - u_{\mathrm{V},i,d,t-1} = v_{\mathrm{V},i,d,t} - z_{\mathrm{V},i,d,t} \tag{55}$$

$$T_{\mathrm{P},i,d,t}^{\mathrm{on}} = u_{\mathrm{P},i,d,t}(T_{\mathrm{P},i,d,t-1}^{\mathrm{on}} + 1) \tag{56}$$

$$T_{\mathrm{V},i,d,t}^{\mathrm{on}} = u_{\mathrm{V},i,d,t}(T_{\mathrm{V},i,d,t-1}^{\mathrm{on}} + 1) \tag{57}$$

$$T_{\mathrm{P},i,\min}^{\mathrm{on}} z_{\mathrm{P},i,d,t} \leq T_{\mathrm{P},i,d,t-1}^{\mathrm{on}} \tag{58}$$

$$T_{\mathrm{V},i,\min}^{\mathrm{on}} z_{\mathrm{V},i,d,t} \leq T_{\mathrm{V},i,d,t-1}^{\mathrm{on}} \tag{59}$$

$$T_{\mathrm{P},i,d,t-1}^{\mathrm{on}} \leq T_{\mathrm{P},i,\max}^{\mathrm{on}}, T_{\mathrm{V},i,d,t-1}^{\mathrm{on}} \leq T_{\mathrm{V},i,\max}^{\mathrm{on}} \tag{60}$$

where $z_{\mathrm{P},i,d,t}$ and $z_{\mathrm{V},i,d,t}$ are the recovery state of peak-shaving and valley-filling DR of customer i at time t on day d, respectively. $T_{\mathrm{P},i,d,t}^{\mathrm{on}}$ and $T_{\mathrm{V},i,d,t}^{\mathrm{on}}$ are the DR duration of peak-shaving and valley-filling DR of customer i at time t on day d, respectively. $T_{\mathrm{P},i,\max}^{\mathrm{on}}$ and $T_{\mathrm{V},i,\max}^{\mathrm{on}}$ are the maximum DR duration of peak-shaving and valley-filling DR of customer i at time t on day d, respectively. $T_{\mathrm{P},i,\min}^{\mathrm{on}}$ and $T_{\mathrm{V},i,\min}^{\mathrm{on}}$ are the minimum DR duration of peak-shaving and valley-filling DR of customer i at time t on day d, respectively. Equations (56)-(59) can be linearized by the Big-M method, which can be respectively converted into

$$\begin{cases} T_{\mathrm{P},i,d,t}^{\mathrm{on}} \geq (T_{\mathrm{P},i,d,t-1}^{\mathrm{on}} + 1) - M_B\left(1 - u_{\mathrm{P},i,d,t}\right) \\ T_{\mathrm{P},i,d,t}^{\mathrm{on}} \leq (T_{\mathrm{P},i,d,t-1}^{\mathrm{on}} + 1) + M_B\left(1 - u_{\mathrm{P},i,d,t}\right) \\ -M_B u_{\mathrm{P},i,d,t} \leq T_{\mathrm{P},i,d,t}^{\mathrm{on}} \leq M_B u_{\mathrm{P},i,d,t} \end{cases} \tag{61}$$

$$\begin{cases} T_{\mathrm{V},i,d,t}^{\mathrm{on}} \geq (T_{\mathrm{V},i,d,t-1}^{\mathrm{on}} + 1) - M_B\left(1 - u_{\mathrm{V},i,d,t}\right) \\ T_{\mathrm{V},i,d,t}^{\mathrm{on}} \leq (T_{\mathrm{V},i,d,t-1}^{\mathrm{on}} + 1) + M_B\left(1 - u_{\mathrm{V},i,d,t}\right) \\ -M_B u_{\mathrm{V},i,d,t} \leq T_{\mathrm{V},i,d,t}^{\mathrm{on}} \leq M_B u_{\mathrm{V},i,d,t} \end{cases} \tag{62}$$

where M_B is a large constant.

4) DR interval time constraints

To ensure the comfort of customers, the interval time between each DR should be longer than the limit in the customer flexibility management contract. The minimum DR interval time limits can be expressed as

$$T_{\mathrm{P},i,d,t}^{\mathrm{off}} = \left(1 - u_{\mathrm{P},i,d,t}\right) \cdot \left(T_{\mathrm{P},i,d,t-1}^{\mathrm{off}} + 1\right) \tag{63}$$

$$T_{\mathrm{P},i,\min}^{\mathrm{off}} v_{\mathrm{P},i,d,t} \leq T_{\mathrm{P},i,d,t-1}^{\mathrm{off}} \tag{64}$$

$$T_{\mathrm{V},i,d,t}^{\mathrm{off}} = \left(1 - u_{\mathrm{V},i,d,t}\right) \cdot \left(T_{\mathrm{V},i,d,t-1}^{\mathrm{off}} + 1\right) \tag{65}$$

$$T_{\mathrm{V},i,\min}^{\mathrm{off}} v_{\mathrm{V},i,d,t} \leq T_{\mathrm{V},i,d,t-1}^{\mathrm{off}} \tag{66}$$

where $T^{\text{off}}_{\text{P},i,d,t}$ and $T^{\text{off}}_{\text{V},i,d,t}$ are DR interval time of peak-shaving and valley-filling DR of customer *i* at time *t* on day *d*. $T^{\text{off}}_{\text{P},i,\min}$ and $T^{\text{off}}_{\text{V},i,\min}$ are the minimum interval time of peak-shaving and valley-filling DR of customer *i* at time *t* on day *d*. Similarly, equations (63)-(66) can be linearized by the Big-M method, which can be respectively converted into

$$\begin{cases} -M_B\left(1-u_{\text{P},i,d,t}\right) \le T^{\text{off}}_{\text{P},i,d,t} \le M_B\left(1-u_{\text{P},i,d,t}\right) \\ T^{\text{off}}_{\text{P},i,d,t} \ge (T^{\text{off}}_{\text{P},i,d,t-1}+1) - M_B u_{\text{P},i,d,t} \\ T^{\text{off}}_{\text{P},i,d,t} \le (T^{\text{off}}_{\text{P},i,d,t-1}+1) + M_B u_{\text{P},i,d,t} \end{cases} \tag{67}$$

$$\begin{cases} -M_B\left(1-u_{\text{V},i,d,t}\right) \le T^{\text{off}}_{\text{V},i,d,t} \le M_B\left(1-u_{\text{V},i,d,t}\right) \\ T^{\text{off}}_{\text{V},i,d,t} \ge (T^{\text{off}}_{\text{V},i,d,t-1}+1) - M_B u_{\text{V},i,d,t} \\ T^{\text{off}}_{\text{V},i,d,t} \le (T^{\text{off}}_{\text{V},i,d,t-1}+1) + M_B u_{\text{V},i,d,t} \end{cases} \tag{68}$$

5) Maximum number of DR constraints

In the customer flexibility management contract of industrial customers, the maximum number of DR in a single day and during a month is generally limited. Therefore, the maximum number of DR constraints can be expressed as

$$\sum_{t=1}^{T} v_{\text{P},i,d,t} \le U^{\text{d}}_{\max,i}, \sum_{t=1}^{T} v_{\text{V},i,d,t} \le U^{\text{d}}_{\max,i} \tag{69}$$

$$\sum_{d=1}^{D_{\text{M}}}\sum_{t=1}^{T} v_{\text{P},i,d,t} \le U^{\text{M}}_{\max,i}, \sum_{d=1}^{D_{\text{M}}}\sum_{t=1}^{T} v_{\text{V},i,d,t} \le U^{\text{M}}_{\max,i} \tag{70}$$

where $U^{\text{d}}_{\max,i}$ and $U^{\text{M}}_{\max,i}$ are maximum number of DR times in a single day and during a month of customer *i,* respectively.

6) Customer uncertainty constraints

Since the improved *N-k* uncertainty model is nonlinear, equations (42)-(43) can be linearized based on robust dual transformation [26] as follows.

$$\left(\lg\partial_{\text{D}} - \sum_{i=1}^{N_{\text{D}}}\lg\left(1-\lambda_i\right)\right)g_t - \sum_{i=1}^{N_{\text{D}}} h_{i,t} \geqslant P^{\text{DSM}}_{d,t} - P^{\text{L}}_{d,t} - P^{\text{m}}_{\text{P},d,t} \tag{71}$$

$$\left(\lg\lambda_i - \lg\left(1-\lambda_i\right)\right)g_t - h_{i,t} \leqslant \sum_{i=1}^{N_D} P^*_{\text{P},i,d,t} - \sum_{i=1}^{N_D} P^*_{\text{V},i,d,t} \tag{72}$$

$$P^*_{\text{P},i,d,t} = u_{\text{P},i,d,t} R^{\text{DRP}}_{i,t} \tag{73}$$

$$P^*_{\text{V},i,d,t} = u_{\text{V},i,d,t} R^{\text{DRP}}_{i,t} \tag{74}$$

where $P^*_{\text{P},i,d,t}$ and $P^*_{\text{V},i,d,t}$ are the actual adjusted load of peak-shaving and valley-filling DR of customer *i* at time *t* on day *d*. g_t and $h_{i,t}$ are dual variables of the robust dual transformation, which $g_t \ge 0, h_{i,t} \ge 0$.

D. Multi-objective optimization solving algorithm based on Tchebycheff decomposition and AHP-entropy weight method

The proposed customer flexibility optimization model for multiple consecutive days includes two objective functions (i.e., customer flexibility management cost and impact index), which should be solved by the multi-objective optimization algorithm. To simultaneously consider the impact of subjective and objective factors on decision-making, an algorithm based on the Tchebycheff decomposition and AHP-entropy weight method is proposed to solve the multi-objective customer flexibility optimization model. Firstly, the Tchebycheff method is utilized to obtain the Pareto frontier solution set by adjusting the weight [28]. The multi-objective function (44) of the customer flexibility optimization model can be converted into

$$\min f_{\text{TF}} = \max_{i\le n}\left\{\alpha_i\left|f_i - f_i^{\text{OP}}\right|\right\} + M_{\text{S}}\sum_{i=1}^{n}\left(f_i - f_i^{\text{OP}}\right) \tag{75}$$

where f_i^{OP} is the ideal objective of f_i . *n* is the total number of objectives in the model, and $n=2$ in this paper. α_i is the weight factor of f_i , and $\sum_{i=1}^{n}\alpha_i = 1$. M_{S} is a minimal constant to avoid the feasible solution space of the model.

Due to the different orders of magnitude of f_1 and f_2 , equation (75) could be normalized as

$$\min f_{\text{TF}} = \max_{i\le n}\left\{\frac{\alpha_i\left|f_i - f_i^{\text{OP}}\right|}{f_i^{\text{NE}} - f_i^{\text{OP}}}\right\} + M_{\text{S}}\sum_{i=1}^{n}\left(f_i - f_i^{\text{OP}}\right) \tag{76}$$

where f_i^{NE} is the negative ideal objective of f_i . For instance, f_1^{NE} is the optimal solution of the single-objective optimization model with f_2 .

The Pareto frontier solution set can be obtained by solving the sub-problem with different weight factors, and considering the subjective and objective impacts on decision-making, a subjective-objective integration weighting method is proposed. Firstly, the subjective weights a_i^{S} are calculated by the AHP method [29], reflecting the decision-makers subjective judgment on the customer flexibility management cost and impact index. Secondly, the objective weights a_i^{O} are computed by the entropy weight method [30] based on the deviation of Pareto solutions. Then, to obtain a more reasonable subjective and objective combined weight of f_i , the subjective-objective combination weight optimization model is built to minimize the total deviation of subjective and objective weights of all Pareto solutions. The objective function of the subjective-objective combination weight optimization model can be expressed as

$$\min H = \sum_{k=1}^{m}\sum_{i=1}^{n}(\omega a_i^{\text{O}} f^*_{i,k} - (1-\omega)a_i^{\text{S}} f^*_{i,k})^2, \tag{77}$$

where H is the total deviation of subjective and objective weights of all Pareto solutions. *m* is the total number of solutions in the Pareto frontier solution set. ω is the subjective-objective weight allocation coefficient. The constraints of the subjective-objective weight allocation coefficient can be expressed as

$$\omega(1-\omega) \ge 0 \tag{78}$$

Then, the optimal subjective-objective combination weight of multi-objectives can be calculated as

$$a_i^{\text{B}} = \omega a_i^{\text{O}} + (1-\omega)a_i^{\text{S}} \tag{79}$$

where a_i^{B} is the optimal combination weight of f_i .

Finally, the multi-objective customer flexibility optimization model should be solved again with the optimal weight a_i^{B}, to obtain the optimal compromise solution of the customer flexibility management. To sum up, the flowchart of the proposed multi-objective customer flexibility optimization solving algorithm is shown in Fig. 3.

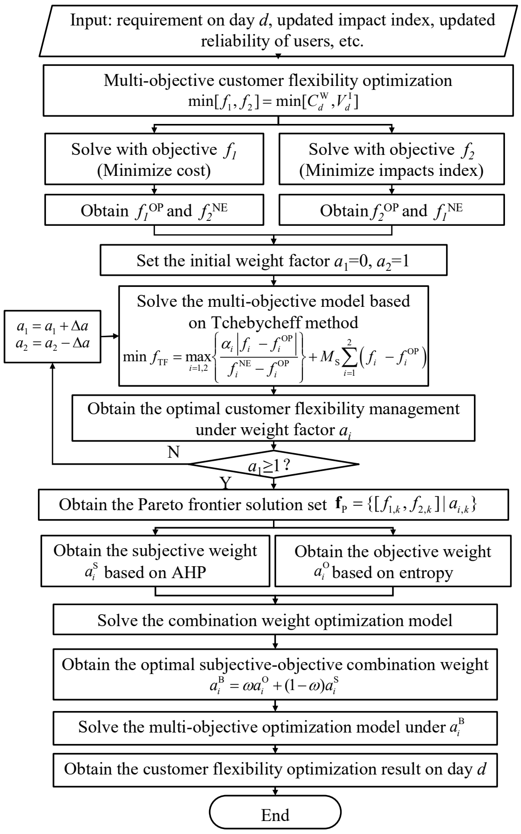

Fig. 3. Flow chart of proposed multi-objective customer flexibility optimization solving algorithm.

IV. Case Studies

To verify the efficiency of the proposed multi-objective customer flexibility optimization for consecutive days of power supply shortages, the historical DR data of manufacturing industrial customers in a city in Zhejiang province, China, are utilized for case studies. The customer flexibility parameters of industrial customers are shown in Table AI. In this case, the total number of industrial customers is 268, and the customers can be divided into five typical power consumption patterns, which are the high power consumption level pattern (U-I), typical peak-avoiding power consumption pattern (U-II), and three basic double-peak power consumption pattern (U-III, U-IV, and U-V) [31]. The customer flexibility potential of customers with typical power consumption patterns is shown in Fig. 4. The maximum flexibility capacity of flexible loads is 2,000kW. Based on the proportion of customer capacity to the load of entire province, the customer flexibility management requirements of the customer flexibility management center are established at 6‰ of the power supply shortages illustrated in Fig. 1. The minimum DR interval time is set to be 2 hours. The unit capacity price for valley-filling DR is 2.0 CNY/kW·day, and the unit electricity price for flexible loads is 4.0 CNY/kWh. Based on the proposed multi-objective optimization solving algorithm, the optimal weight coefficients of the two objective functions of customer flexibility management cost and impact on production are 0.548 and 0.452, respectively. The proposed model is a mixed-integer linear programming problem (MILP), and the optimization process is carried out on a PC with 16GB of RAM and AMD Ryzen5 @ 3.60 GHz processor using Gurobi 9.5.0 solver and MATLAB 2019b software, and the computation time is average 3,536s.

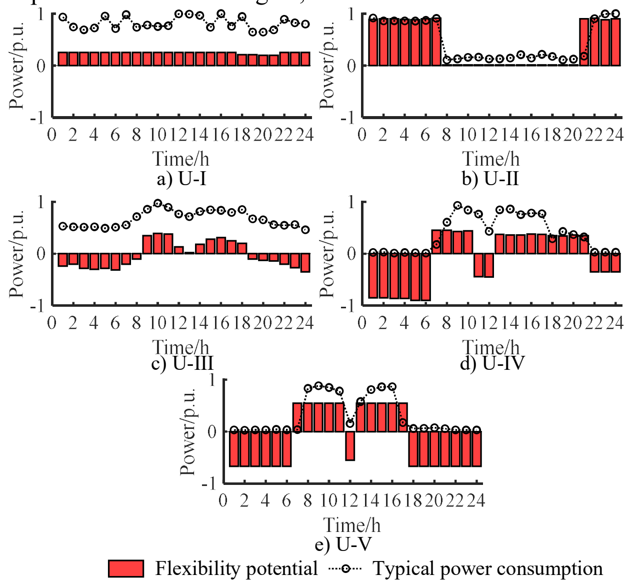

Fig. 4. Flexibility potential of customers with typical power consumption patterns.

A. Optimization results of customer flexibility management over consecutive days

To verify the efficiency of the proposed customer flexibility management method over multiple consecutive days (MT-M) in addressing consecutive days of power supply shortages, the customer flexibility management results are compared with the optimization results using a price-based scheduling method (PB-M) [14]. The total customer flexibility management costs, impacts index, and loss of load in optimal results of MT-M and PB-M are shown in Table I. The flexibility management results of customers with similar consumption patterns are presented, and the optimal customer flexibility management for different types of customers are shown in Fig. 5.

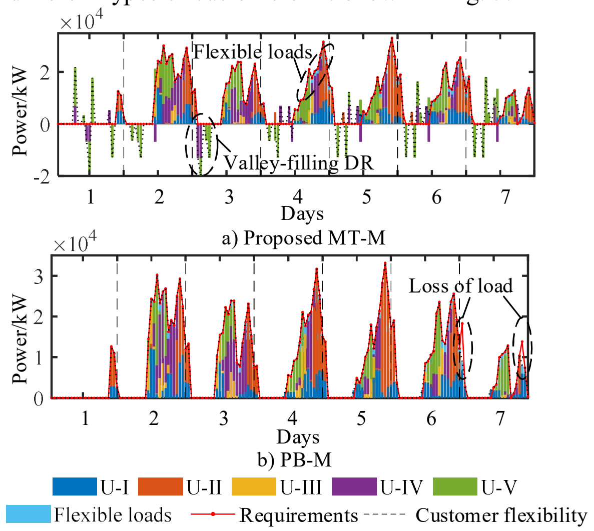

Fig. 5 Optimization results of customer flexibility management over consecutive days.

TABLE I
OPTIMIZATION RESULTS OF THE PROPOSED MT-M AND PB-M

Optimization results	Proposed MT-M	PB-M [14]
Costs/10^6·CNY	4.19	2.83
Impacts index/10^6·CNY	1.76	14.26
Loss of load/kWh	0	15731
Peak-shaving DR/10^5·kWh	15.07	13.15
Valley-filling DR/10^5·kWh	2.55	0
Flexible load DR/10^5·kWh	0.71	0.51

It can be seen from Table I that, compared with PB-M, the proposed MT-M could effectively reduce the loss of load during seven consecutive days of power supply shortages. The total customer flexibility management cost of the proposed MT-M is 4,198,898 CNY, with a production impact factor of 1,763,517 CNY. Compared to the results of PB-M, there was an increase in customer flexibility management costs by 32.46%, while the production impact was reduced by 79.63%. It can be seen from Fig. 5 that, compared to PB-M, a more significant amount of flexible load resources is scheduled in the proposed MT-M, with an average additional scheduling of 39.2%. Although the cost of flexible load resources exceeds that of industrial customers, leading to an increase in customer flexibility management costs, it reduced the impact index for production interruptions of industrial customers during multiple consecutive days of customer flexibility management. Furthermore, the valley-filling DR of U-IV and U-V, scheduled in the proposed MT-M during periods without power supply shortages, also helped to reduce the impact index for production. In PB-M, the optimization focuses on minimizing the customer flexibility management cost without considering the impact on industrial production. As a result, the optimization results do not engage in valley-filling DR to reduce the associated costs. In the optimization results of the proposed MT-M, after seven consecutive days of customer flexibility management, 34.7% of industrial customers did not reach the maximum number of DR in their contracts, which is 38.8% higher than that in the optimization results of PB-M. Consequently, the proposed MT-M can enhance customer flexibility and reduce power supply shortages in the later stages of consecutive days of heatwaves.

However, in the customer flexibility management results of PB-M, it is observed that not all customers achieve their DR frequency limits, yet the customer flexibility management center still can not meet the requirements. Industrial customers are categorized into three tiers based on their power capacity to analyze the customer flexibility management for different customers during consecutive days of power shortages further. The proportions of DR frequencies for different customer categories within the customer flexibility optimization results of MT-M and PB-DR, along with the probabilities of invitation confirmations, are shown in Fig. 6.

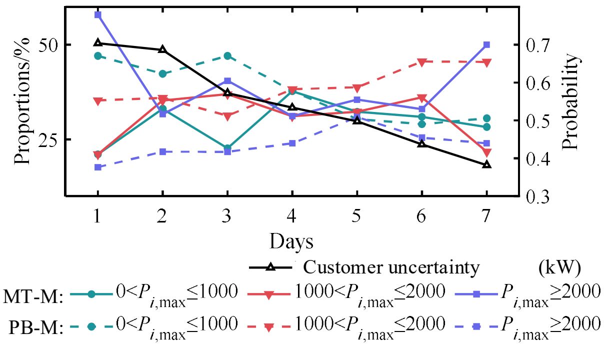

Fig. 6 Adjusted frequencies and customer uncertainty over consecutive days.

It can be seen from Fig. 6 that, in the customer flexibility management results of the proposed MT-M, the proportion of DR frequency of large-scale customers (i.e. $P_{i,\max} \geq 2000\text{kW}$) is 40.87% higher than that in PB-M, with a trend of fluctuating decline as the duration of power supply shortages increases. Two primary reasons account for this result. Firstly, as the consecutive days of customer flexibility management extend, the probability of invitation confirmations gradually decreases from an average of 0.70 to 0.53. The proposed industrial customer uncertainty updating and modeling method enables the identification of changes in customer uncertainty, reducing the dispatch frequency of large-scale customers. Therefore, the loss of load caused by the uncertainty of large-scale customers in the later stages of consecutive power supply shortages. Secondly, reducing the customer flexibility management of small-scale customers allows more small-scale customers to participate in customer flexibility management during the later stages of consecutive power supply shortages, achieving a closer alignment with requirements for the customer flexibility management center. In summary, the proposed MT-M could reduce the impact of consecutive days of customer flexibility management on customer production and adjust strategies based on customer uncertainty to decrease the loss of load during consecutive days of power supply shortages.

B. Comparison of different customer flexibility optimization models

To verify the impact of considering the consecutive days of power supply shortages on the customer flexibility optimization, the proposed MT-M is compared with the customer flexibility optimization model for a single day (nMT-M) [20], and the customer flexibility optimization model considering the *N-k* uncertainty (*N-k*-M) [26]. Due to significant variations in daily requirements in actual scenarios, analyzing the trends of each parameter over consecutive days presents specific challenges. Hence, in this case, the consecutive days of customer flexibility management requirements are created by replicating the power supply shortages from the 2nd day in Fig. 1. The loss of load, customer flexibility management cost (excluding the cost of lost load), and impact on production of different customer flexibility optimization models for 7 days of power supply shortages are shown in Fig. 7.

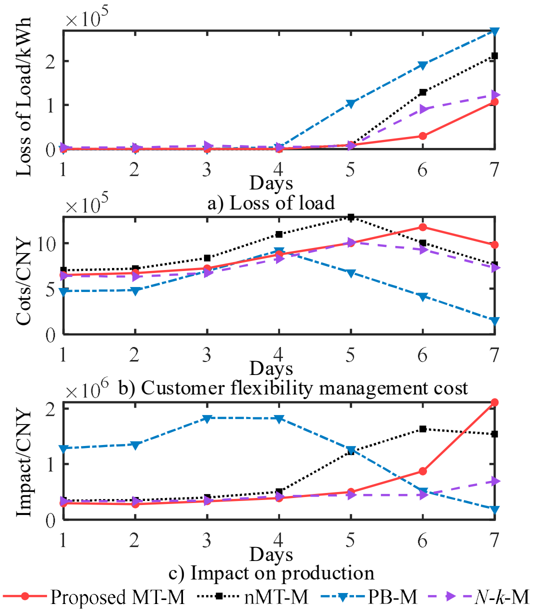

Fig. 7 Comparison of optimization results in different customer flexibility optimization models.

It can be seen from Fig. 7 that, compared with other customer flexibility optimization models, the proposed MT-M could reduce and delay the loss of load and impact on production over consecutive days, while not significantly increasing customer flexibility management costs. In this case, the loss of load in the PB-M method surged starting from the 5th day, totaling 569,317 kWh, while the losses in the MT-M and *N*-*k*-M methods began to increase from the 6th day, amounting to 349,605 kWh and 239,071 kWh, respectively. Compared to nMT-M, *N*-*k*-M, and PB-M, the proposed method reduces the loss of load by 58.44%, 39.23%, and 74.48%, respectively, over consecutive days. The average customer flexibility management cost in the proposed MT-M is 2.79 CNY/kWh, which is 0.16 CNY/kWh lower than that in nMT-M, and 1.03 CNY/kWh and 0.29 CNY/kWh higher than that in PB-M and *N*-*k*-M, respectively. However, due to a substantial occurrence of load losses, it becomes less economical for the customer flexibility management center.

Compared to *N*-*k*-M, the occurrence of scheduling the customer with high DR participation uncertainty ($\lambda_{i,d} \geqslant 0.3$) was reduced by 10.0% in the proposed MT-M. This indicates that the improved *N*-*k* uncertainty, which considers the differences in customers participation uncertainty, can reduce the engagement of high-uncertainty customers as customer participation uncertainty gradually increases. As a result, the reliability of customer flexibility management and power systems could be enhanced. Furthermore, compared to nMT-M, the occurrence of scheduling the same customer on two consecutive days was reduced by 3.7% during the 1st-4th days in the proposed MT-M. This indicates that considering the impact of consecutive customer flexibility management on customer production allows for a more equitable distribution of flexibility management among customers over consecutive days, further reducing the impact on customer production.

In summary, for short-term consecutive power supply shortages (within 4 days in this case), PB-M is capable of meeting the customer flexibility requirement at the lowest cost without is capable of meeting. However, for more extended periods of consecutive power supply shortages (exceeding 5 days in this case), with the adoption of multi-objective optimization considering the impacts index over consecutive days and the uncertainty updating and modeling method, the proposed customer flexibility optimization facilitates more balanced scheduling of industrial customers. On this basis, the customer flexibility optimization could help customer flexibility management centers reduce and delay the power supply shortages during consecutive days of heatwaves.

V. Conclusion

To address the issue of optimizing the scheduling of limited demand-side resources during consecutive days of power supply shortages caused by extreme weather, a multi-objective customer flexibility optimization model for customer flexibility management centers is proposed in this paper. In this model, the optimization objectives are to minimize customer flexibility management costs and the impact index on production. Before optimization, an exponential smoothing-based data updating method for the impact index and a Bayesian inference-based data updating method for customer uncertainty is proposed. Simulation results show that the proposed method can significantly reduce the loss of load during consecutive days of power supply shortages (from 15,731 kWh to 0 in the proposed case based on an actual heatwave). Due to the updating of impact index and customer uncertainty, the risk of load loss and the impact on production at the later stages of consecutive power supply shortages can be reduced and delayed. While the results demonstrate the proposed model's potential to enhance the reliability and flexibility of the power system during extreme weather conditions, further research is needed to improve the practical implementation. In this paper, the nonlinear relationship between reduced load and impact on production, as well as the variability of customer uncertainty, is taken into account in customer flexibility management. Future work could explore dynamic pricing mechanisms for different types of industrial customers and consider factors such as product type, scale, the number of production lines, and order status to evaluate their impact on the consecutive days of profit losses for industrial customers, thereby achieving more refined customer flexibility management.

VI. Appendix A

TABLE AI
Load Flexibility Parameters of Industrial Customers

No.	Capacity (kW)	Pattern	$T^{\text{on}}_{i,\max/m}$ (h)	$c^{\text{p}}_{\text{P},i,t}$ (CNY/kWh)	$Q_{i,d}$ (kWh)	$\mu^{\text{H}}_{i,0}$	$\varepsilon^{\text{H}}_{i,0}$
1	1415.3	U-I	4/2	3.00	19944.2	18	2
2	1057.9	U-I	4/2	1.50	14318.0	20	0
3	827.4	U-I	4/2	2.00	13542.6	19	1
4	2304.1	U-I	4/2	2.71	40371.2	17	3
5	1344.7	U-I	4/2	2.00	21275.2	19	1
6	1058.1	U-I	4/2	2.22	15758.1	19	1
7	5379.3	U-I	4/2	2.00	64001.0	17	3
8	593.1	U-I	4/2	1.89	7686.6	19	1
9	1306.3	U-I	4/2	2.00	17382.3	19	1
10	500.3	U-I	4/2	2.60	10056.3	19	1
11	4872.6	U-II	4/1	3.00	39624.1	18	2
12	1192.8	U-II	4/1	1.50	10545.2	17	3
13	1120.6	U-II	4/1	2.00	9754.8	17	3

No.	Capacity (kW)	Pattern	$T^{\mathrm{on}}_{i,\max/\mathrm{m}}$ (h)	$c^{\mathrm{P}}_{\mathrm{P},i,t}$ (CNY/kWh)	$Q_{i,d}$ (kWh)	$\mu^{\mathrm{H}}_{i,0}$	$\varepsilon^{\mathrm{H}}_{i,0}$
14	759.3	U-II	4/1	2.71	7713.0	18	2
15	1448.1	U-II	4/1	2.00	17105.0	20	0
16	1257.0	U-II	4/1	2.22	11730.6	19	1
17	730.1	U-II	4/1	2.00	7593.8	17	3
18	737.6	U-II	4/1	1.89	7726.3	19	1
19	836.4	U-II	4/1	2.00	7183.9	19	1
20	5248.4	U-II	4/1	2.60	39480.4	17	3
21	945.5	U-III	4/1	3.81	13097.3	19	1
22	556.1	U-III	4/1	1.20	8212.6	19	1
…	…	…	…	…	…	…	…
265	809.2	U-V	2/1	2.71	5720.6	6	2
266	2504.4	U-V	2/1	2.00	19854.6	6	5
267	2400.1	U-V	2/1	2.22	2409.8	6	4
268	1049.9	U-V	2/1	3.99	3268.9	6	4

* Full data is available in the supporting document.

VII. References

[1] V. Thompson, A. T. Kennedy-Asser, E. Vosper, *et al.*, "The 2021 western North America heat wave among the most extreme events ever recorded globally," *Sci. Adv.*, vol. 8, no. 18, p. eabm6860, May 2022.

[2] M. O. Molina, C. Gutiérrez, M. Ortega, *et al.*, "Summer heatwaves, wind production and electricity demand in Southern Europe: climatic conditions and impacts," *Environ. Res. Commun.*, vol. 5, no. 8, p. 085005, Aug. 2023.

[3] F. Meng, L. Zhang, G. Ren, *et al.*, "Impacts of UHI on variations in cooling loads in buildings during heatwaves: A case study of Beijing and Tianjin, China," *Energy*, vol. 273, p. 127189, Jun. 2023.

[4] Q. Shi, C.-F. Chen, A. Mammoli, *et al.*, "Estimating the Profile of Incentive-Based Demand Response (IBDR) by Integrating Technical Models and Social-Behavioral Factors," *IEEE Transactions on Smart Grid*, vol. 11, no. 1, pp. 171–183, Jan. 2020.

[5] Y. Dong, X. Xie, K. Wang, *et al.*, "An Emergency-Demand-Response Based Under Speed Load Shedding Scheme to Improve Short-Term Voltage Stability," *IEEE Transactions on Power Systems*, vol. 32, no. 5, pp. 3726–3735, Sep. 2017.

[6] H. A. Aalami, M. P. Moghaddam, and G. R. Yousefi, "Demand response modeling considering Interruptible/Curtailable loads and capacity market programs," *Applied Energy*, vol. 87, no. 1, pp. 243–250, Jan. 2010.

[7] W. Xu, D. Zhou, X. Huang, *et al.*, "Optimal allocation of power supply systems in industrial parks considering multi-energy complementarity and demand response," *Applied Energy*, vol. 275, p. 115407, Oct. 2020.

[8] T. Lu, Z. Wang, J. Wang, Q. Ai and C. Wang, "A data-driven Stackelberg market strategy for demand response-enabled distribution systems," *IEEE Trans. Smart Grid*, vol. 10, no. 3, pp. 2345-2357, May 2019.

[9] S. Maharjan, Q. Zhu, Y. Zhang, *et al.*, "Dependable Demand Response Management in the Smart Grid: A Stackelberg Game Approach," *IEEE Trans. Smart Grid*, vol. 4, no. 1, pp. 120–132, Mar. 2013.

[10] Z. Xu, D. S. Callaway, Z. Hu, *et al.*, "Hierarchical Coordination of Heterogeneous Flexible Loads," *IEEE Transactions on Power Systems*, vol. 31, no. 6, pp. 4206–4216, Nov. 2016.

[11] M. H. Shoreh, P. Siano, M. Shafie-khah, *et al.*, "A survey of industrial applications of Demand Response," *Electric Power Systems Research*, vol. 141, pp. 31–49, Dec. 2016.

[12] H. Golmohamadi, R. Keypour, B. Bak-Jensen, *et al.*, "A multi-agent based optimization of residential and industrial demand response aggregators," *International Journal of Electrical Power & Energy Systems*, vol. 107, pp. 472–485, May 2019.

[13] M. Z. Oskouei, S. Zeinal-Kheiri, B. Mohammadi-Ivatloo, *et al.*, "Optimal Scheduling of Demand Response Aggregators in Industrial Parks Based on Load Disaggregation Algorithm," *IEEE Systems Journal*, vol. 16, no. 1, pp. 945–953, Mar. 2022.

[14] R. Lu, R. Bai, Y. Huang, *et al.*, "Data-driven real-time price-based demand response for industrial facilities energy management," *Applied Energy*, vol. 283, p. 116291, Feb. 2021.

[15] Y. M. Ding, S. H. Hong, and X. H. Li, "A Demand Response Energy Management Scheme for Industrial Facilities in Smart Grid," *IEEE Transactions on Industrial Informatics*, vol. 10, no. 4, pp. 2257–2269, Nov. 2014.

[16] A. Gholian, H. Mohsenian-Rad, and Y. Hua, "Optimal Industrial Load Control in Smart Grid," *IEEE Transactions on Smart Grid*, vol. 7, no. 5, pp. 2305–2316, Sep. 2016.

[17] X. Zhang, G. Hug, J. Z. Kolter, *et al.*, "Demand Response of Ancillary Service From Industrial Loads Coordinated With Energy Storage," *IEEE Transactions on Power Systems*, vol. 33, no. 1, pp. 951–961, Jan. 2018.

[18] Q. Lu and Y. Zhang, "A multi-objective optimization model considering users' satisfaction and multi-type demand response in dynamic electricity price," *Energy*, vol. 240, p. 122504, Feb. 2022.

[19] H. Chen, L. Gao, and Z. Zhang, "Multi-objective optimal scheduling of a microgrid with uncertainties of renewable power generation considering user satisfaction," *International Journal of Electrical Power & Energy Systems*, vol. 131, p. 107142, Oct. 2021.

[20] H. Sheng, C. Wang, B. Li, *et al.*, "Multi-timescale Active Distribution Network Scheduling Considering Demand Response and User Comprehensive Satisfaction," *IEEE Transactions on Industry Applications*, vol. 57, no. 3, pp. 1995–2005, May 2021.

[21] J. Zhang, P. Zhang, H. Wu, *et al.*, "Two-stage load-scheduling model for the incentive-based demand response of industrial users considering load aggregators," *IET Generation, Transmission & Distribution*, vol. 12, no. 14, pp. 3518–3526, 2018.

[22] V. Thompson, A. T. Kennedy-Asser, E. Vosper, *et al.*, "The 2021 western North America heat wave among the most extreme events ever recorded globally," *Sci. Adv.*, vol. 8, no. 18, p. eabm6860, May 2022.

[23] D. Wu, Y. Wang, L. Li, *et al.*, "Demand response ability evaluation based on seasonal and trend decomposition using LOESS and S–G filtering algorithms," *Energy Reports*, vol. 8, pp. 292–299, Aug. 2022.

[24] E. S. Gardner, "Exponential smoothing: The state of the art—Part II," *International Journal of Forecasting*, vol. 22, no. 4, pp. 637–666, Oct. 2006.

[25] P. M. Castro, I. Harjunkoski, and I. E. Grossmann, "New Continuous-Time Scheduling Formulation for Continuous Plants under Variable Electricity Cost," *Ind. Eng. Chem. Res.*, vol. 48, no. 14, pp. 6701–6714, Jul. 2009.

[26] Q. Wang, J.-P. Watson, and Y. Guan, "Two-stage robust optimization for *N-k* contingency-constrained unit commitment," *IEEE Trans. Power Syst.*, vol. 28, no. 3, pp. 2366-2375, 2013.

[27] Z. Gao, J. Tao, D. Zhou, *et al.*, "Efficient Parametric Yield Estimation Over Multiple Process Corners via Bayesian Inference Based on Bernoulli Distribution," *IEEE Transactions on Computer-Aided Design of Integrated Circuits and Systems*, vol. 39, no. 10, pp. 3144–3148, Oct. 2020.

[28] X. Ma, Q. Zhang, G. Tian, *et al.*, "On Tchebycheff Decomposition Approaches for Multiobjective Evolutionary Optimization," *IEEE Transactions on Evolutionary Computation*, vol. 22, no. 2, pp. 226–244, Apr. 2018.

[29] H. Gao, J. Yang, S. He, *et al.*, "Decision-making method of sharing mode for multi-microgrid system considering risk and coordination cost" *J. Modern Power Syst. Clean Energy,* vol. 10, no. 6, pp. 1690-1703, Nov. 2022.

[30] Y. Zhu, D. Tian, and F. Yan, "Effectiveness of Entropy Weight Method in Decision-Making," *Mathematical Problems in Engineering*, vol. 2020, p. e3564835, Mar. 2020.

[31] F. Lu, X. Cui, J. Xing, *et al.*, "Electricity Load Profile Characterisation for Industrial Users Based On Normal Cloud Model and iCFSFDP Algorithm," *IEEE Transactions on Power Systems*, vol. 38, no. 4, pp. 3799–3813, Jul. 2023.

Yunchu Wang (Student Member, IEEE) received the B.E. degree in electrical engineering from Zhejiang University, Hangzhou, China, in 2020. She is currently pursuing the Ph.D. degree with the College of Electrical Engineering, Zhejiang University. Her research interests include power system economics and optimization, and demand response.

Feng Lu received the master's degree in electrical engineering in 2011 from Zhejiang University, Hangzhou, China, where he is currently working toward the Ph.D. degree with the College of Electrical Engineering. His research interests include demand response and power retail management.

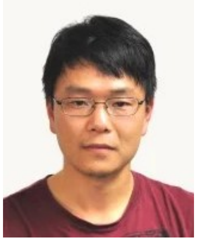

Chenghong Gu (Member, IEEE) received the master's degree in electrical engineering from Shanghai Jiao Tong University, Shanghai, China, in 2007, and the Ph.D. degree from the University of Bath, Bath, U.K. He is currently a Professor and EPSRC Fellow with the Department of Electronic and Electrical Engineering, University of Bath. His research interests include multivector energy system, smart grid, and power economics.

Li Yang (Member, IEEE) received the Ph.D. degree in electrical engineering from Zhejiang University, Hangzhou, China, in 2004. She held a postdoctoral position at the Department of Electrical Engineering, Turin Polytechnic University, from 2007 to 2008. She is currently an Associate Professor with the College of Electrical Engineering, Zhejiang University. Her research interests include power market, power system economics, and distribution network planning.

Zhenzhi Lin (Senior Member, IEEE) received the Ph.D. degree in electrical engineering from the South China University of Technology, Guangzhou, China, in 2008. From 2007 to 2008, he was a Research Assistant with the Department of Electrical Engineering, The Hong Kong Polytechnic University, Hong Kong, China, a Research Scholar with the Department of Electrical Engineering and Computer Science, University of Tennessee, Knoxville, USA, from 2010 to 2011, and a Research Associate with the College of Engineering and Computing Sciences, Durham University, Durham, U.K., from 2013 to 2014. He is currently a Professor with the College of Electrical Engineering, Zhejiang University, Hangzhou, China. His research interests include power system situational awareness, power system restoration, power system economics, data mining, and artificial intelligence applications in power systems.

Ming Wu received the Ph.D. degree from the University of Chinese Academy of Sciences. He is currently with the China Electric Power Research Institute, Beijing, China. His research interests are about microgrid control and renewable energy integration.

Liangzhou Yao (Fellow, IEEE) is currently the Director of Smart Grid Research Institute, and a Professor with the School of Electrical Engineering and Automation, Wuhan University, China. Prior to joining the Wuhan University in 2018, he was the Vice President and Honorary Chief Engineer with China Electric Power Research Institute during 2012–2018, Vice President with State Grid Electric Power Research Institute during 2011–2012, Department Head and Senior Expert with Alstom Grid Research & Technology Centre in the U.K. during 2004–2011, Senior Power System Analyst with ABB U.K. Ltd. during 1999–2004, Postdoctoral Research Associate with the University of Manchester during 1995–1999, and Postdoctoral Research Fellow and an Associate Research Professor with Tsinghua University during 1993–1995, respectively. His research interests include renewable energy grid integration and control, energy storage grid integration and control, power electronics converter control, and HVDC and DC grid technologies. He is also a Member of Academia Europaea, and a Fellow of IET and AAIA.